This project has received funding from the Euratom research and training programme 2014-2018 under grant agreement No 662287.

EJP-CONCERT

European Joint Programme for the Integration of Radiation Protection Research

H2020 – 662287

D 9.48 – Histopathological analyses

Lead Author: HMGU and ENEA

With contributions from: All project partners (DH-PHE, HMGU, ENEA, DU, OBU) and Advisory Board members

Reviewer(s): CONCERT coordination team

Work package / Task	**WP 9** **Task 9.2**	**SST9.2.3.1**
Deliverable nature:	**(Draft) manuscript**	
Dissemination level: (Confidentiality)	**Public**	
Contractual delivery date:	**Month 30 (CONCERT M52)**	
Actual delivery date:	**Month 30 (CONCERT M52)**	
Version:	**1**	
Total number of pages:	**12**	
Keywords:	**Ionising Radiation; Lens; Cataract; Mouse Models, Histopathology**	
Approved by the coordinator:	**M52**	
Submitted to EC by the coordinator:	**M52**	

Abstract

The lens of the eye is known to be more radiosensitive than previously thought but, despite a substantial reduction in occupational dose limits in line with an assumed threshold of 0.5 Gy for cataract formation, based on recent epidemiological information and reanalyses, the mechanisms of low dose radiation cataract induction are still unclear. This is an important current public health issue, for instance for medical radiation workers, many of whom will need to amend their working practices despite a clear understanding of the effects of chronic, low dose, ionising radiation exposure.

The LDLensRad project aims to bring together experts from across Europe to answer a number of key research questions on this topic, including: how does low dose radiation cause cataracts; is there a dose rate effect, and how does genetic background influence cataract development after radiation exposure. CONCERT Deliverable 9.48, 3.1 of the project, describes the work done to date looking at global radiosensitivity in terms of histopathological and neurological effects.

CONTENT

1. HISTOPATHOLOGY AT HMGU ---- 4

Methodology ---- **4**

B6C3F1 mice ---- **4**

C57BL/6J mice ---- **4**

129/Sv mice ---- **4**

2 CONCLUSIONS ---- 5

3 LENS AS AN INDICATOR OF GLOBAL RADIOSENSITIVITY – ENEA RESULTS ---- 6

Neurogenesis evaluation ---- **6**

Evaluation of lens opacity ---- **8**

4 CONCLUSIONS ---- 10

1. Histopathology at HMGU

Methodology

Mice of 3 strains, (C57BL/6JG x C3HeB/FeJ)F1 (B6C3F1), C57BL/6J and 129/Sv mice from HMGU and PHE were analysed for histological changes at different endpoints. Up to now histological analyses were done for B6C3F1 and C57BL/6J mice sacrificed 20 months after irradiation, as well as 129/Sv sacrificed 12 months after irradiation. B6C3F1 mice were statistically analysed for sex, mouse line and dose, C57BL/6J mice for dose and dose dependent changes, but 129/Sv mice only for dose rate differences. Eye lenses were fully examined, with a special focus on alteration at the posterior and anterior pole and sutures as well as the cortical region.

B6C3F1 mice

Histological analyses of B6C3F1 mice 20 months after irradiation revealed a linear dependency of applied dose and posterior subcapsular cataract (PSC) occurrence (Tab. 1.1, columns 7-9). This relationship appears to be independent of sex and genotype. PSC developed in controls with a frequency around 20%, whereas 60-80% of the 2 Gy-irradiated mice developed PSC. Nearly all of the 2Gy-irradiated lenses showed some opacification. Anterior lesions appeared in a less regular pattern. Occurrence of anterior subcapsular cataracts (ASC) or lesions of the anterior inner cortex was not dose-dependent (Tab. 1.1, columns 10-12). ASCs appeared in controls as often as PSCs.

Posterior as well as anterior sutures were composed of enlarged fibre cells around the suture, intercellular spaces, and either pervaded with an aqueous/ a proteinaceous liquid or air, pseudo-epithelial cells directly below the capsule and debris of fibre cells (Fig. 1.1, A+B).

C57BL/6J mice

These inbred mice mirrored the results of the B6C3F1 hybrids (Tab. 2). PSCs occurred in a dose-dependent manner with a peak frequency of 80% in both dose rate groups irradiated with 2 Gy. Like lenses of B6C3F1 mice, the overall condition of the C57BL/6J lenses was normal, besides the posterior and anterior alterations.

129/Sv mice

Unirradiated control 129/Sv mice were remarkably different compared to other mouse strains such as C57BL/6J and B6C3F1 mice (Fig. 1.2). All examined lenses were characterized by a thinner cortical region at the posterior pole compared to the anterior pole, with the appearance of a posterior dislocation of the lens nucleus. The perinuclear fibre cells were not well-differentiated and unable to form a regular posterior cortex. On the contrary, anterior cortices looked normal if no suture-related lesion developed. Posterior lesions did not form in these lenses after irradiation, instead, anterior lesions appeared more frequently after irradiation in 129/Sv mice. No control mice displayed these anterior lens changes (Table 1.2).

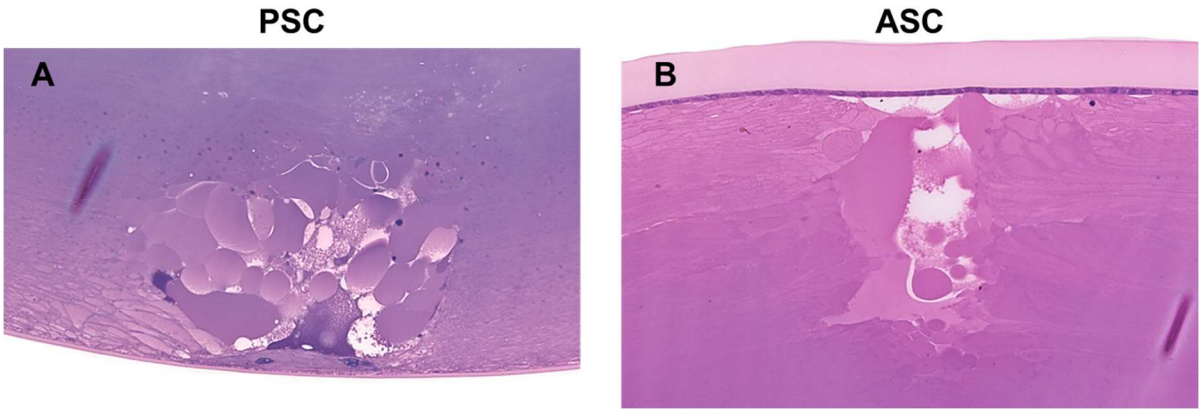

Figure 1.1: Lesions in B6C3F1 and C57BL/6J mice. Posterior subcapsular cataract **(A)**. Anterior subcapsular cataract **(B)**.

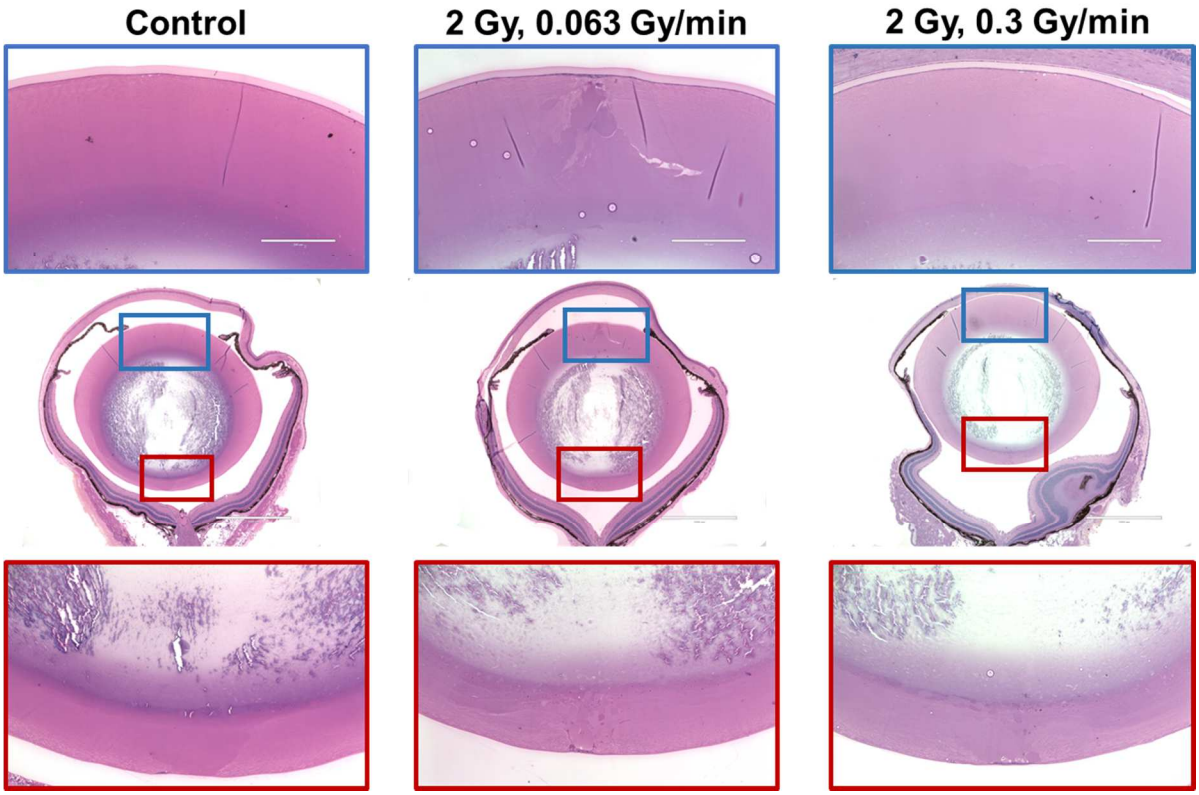

Figure 1.2: Lens histology of 129/Sv mice.

1 Conclusions

Histology revealed the immense impact of genotype on lens conditions. The C57BL/6J or B6C3F1 lenses, exposed to 2 Gy, showed a less severe phenotype than unirradiated 129/Sv control mice. Unfortunately, no optical coherence tomography (OCT) examinations could be done in 129/Sv mice, but based on previous *in vivo* OCT measurements in neonatal irradiated mice, it can be assumed that these lenses would be imaged as highly scattering samples. The structures covering the inner posterior cortex might lead to a highly light scattering area in OCT. The assumption that radiation-induced cataracts are mainly located at the posterior lens cannot be fully confirmed for all mouse strains in this study. PSCs and ASCs occurred in a dose-dependent indeed (though dose dependence has to be further documented with more samples). Surprisingly, anterior lesions constituted a more reliable feature of radiation exposure, especially in the 129/Sv strain. The disorder of the posterior inner cortex in 129/Sv mice might have had

an impact on the fibre cell structure around the suture, which would explain the relatively higher occurrence of PSC's in 129/Sv controls compared to C57BL/6J or B6C3F1 controls.

2 Lens as an indicator of Global Radiosensitivity – ENEA results

Ptch1$^{+/-}$ mice, representing a mouse model of the Gorlin syndrome, exhibit a marked radiation hypersensitivity that suggests a role for *Ptch1* in the response to ionizing radiation. Besides a dramatic tumor predisposition to radiogenic cancer, *Ptch1*$^{+/-}$ mice are also a relevant radiation-induced cataract mouse model and exhibit neurogenesis defects. The goal of WP3 is to test the hypothesis of the lens as an indicator of global radiosensitivity. Since individual mutations are strongly modulated by the host genetic background and marked strain-dependent differences in response to radiation exposures exist, to investigate the contribution of genetic background to the radiation risk for non-cancer diseases, *Ptch1*$^{+/-}$ mice have been bred on two different genetic backgrounds (CD1 and C57Bl/6). Mice were then whole-body irradiated with 2 Gy of γ-rays (^{60}Co) at postnatal day 2 (P2) or at 10 weeks (10W) of age and examined for defects in hippocampal neurogenesis and cataract.

Neurogenesis evaluation

Irradiation at P2: Brains from WT and *Ptch1*$^{+/-}$ mice (*Ptch1*$^{+/-}$/CD1, CD1, *Ptch1*$^{+/-}$/Bl6 and C57Bl6) of 6 weeks of age, that have been irradiated with 2 Gy of γ-rays (0.3 Gy/min) at postnatal day 2 (P2), were collected for histopathological analyses with stage-specific neurogenesis markers (Figure 1A).

A.

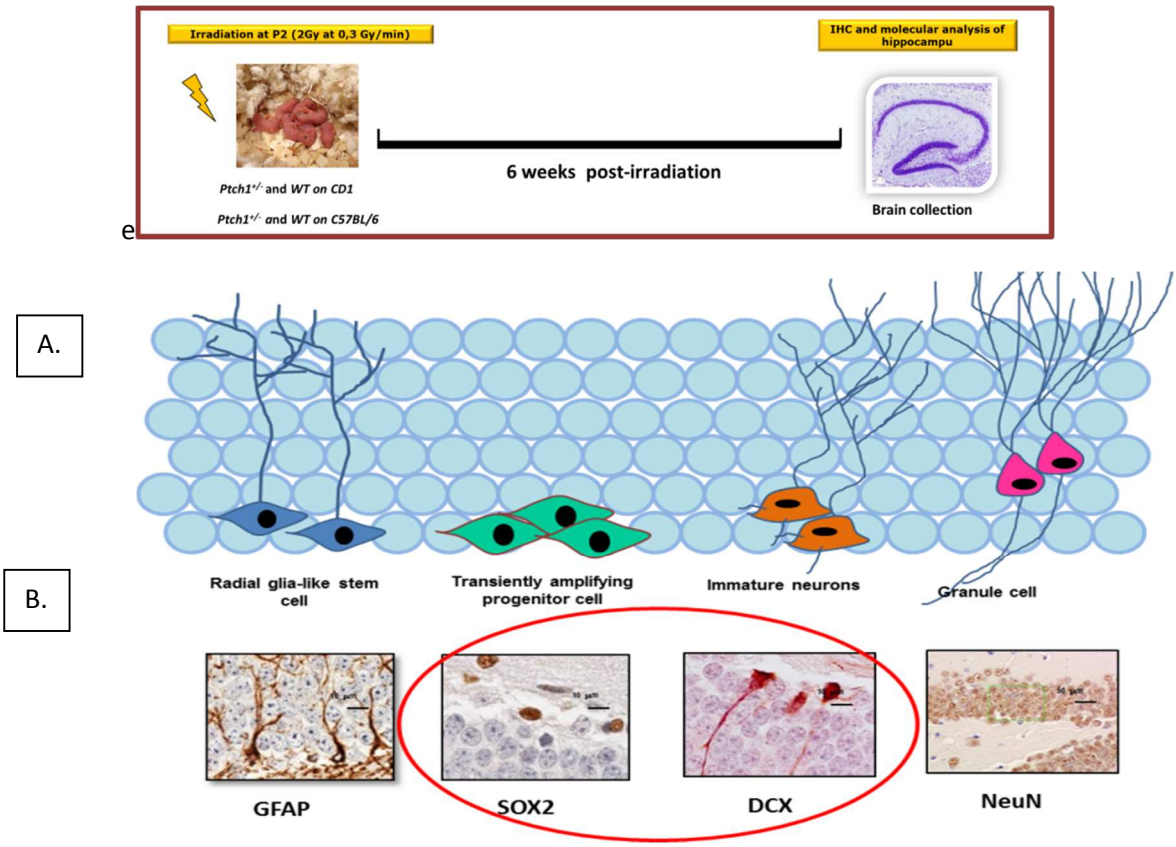

Figure 2.1: (A) Experimental scheme. (B) Schematic representation of adult hippocampal neurogenesis. Red circle marks the two cell populations evaluated.

Hippocampus neurogenesis is a multistep process occurring throughout life, consisting in the generation of new functional granule neurons from adult neural stem cells through the amplification of intermediate progenitors and neuroblasts, as well as the integration of these new neurons into the existing neural circuits. The different cellular populations in the dentate gyrus are distinguishable for their morphology and expression of stage-specific cellular markers. We have evaluated the radiation-dependent modifications in the cellular composition of the sub granular zone of the dentate gyrus applying a criterion based on a combination of morphological cellular features and immunohistochemical labelling. In particular, we have immunostained for Sox2 and Dcx, labelling progenitor cells and immature neurons, respectively (Figure 1B).

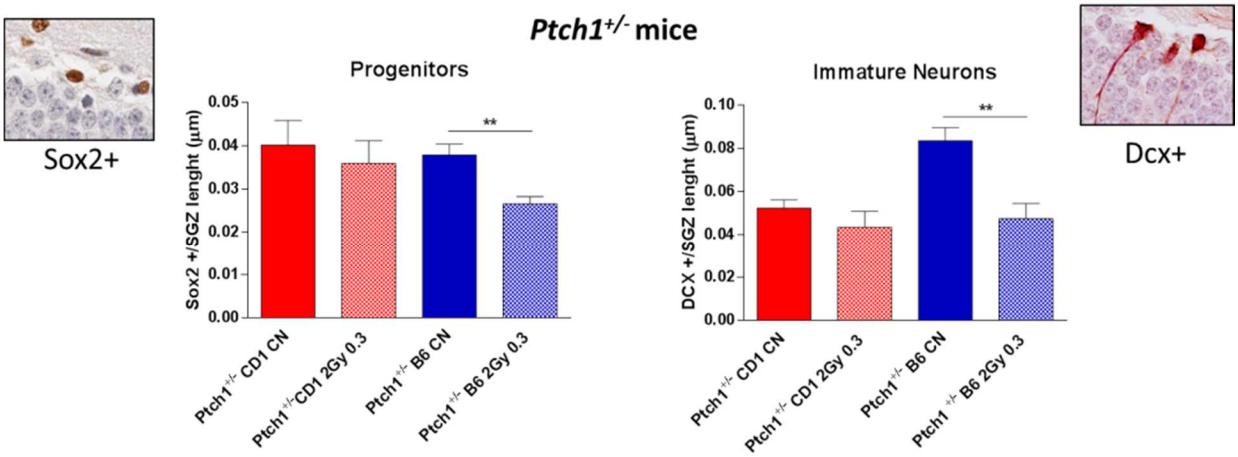

Figure 2.2: Evaluation of the effect of P2-irradiation on hippocampal neurogenesis

While neonatal irradiation with 2 Gy of γ-rays (0.3 Gy/min) did not cause any defect in *Ptch1*$^{+/-}$/CD1 mice, persistent impairment of Sox2 and Dcx populations was detected in *Ptch1*$^{+/-}$/Bl6 mice at 6 weeks post-irradiation (Figure 2). This suggest that the overall sensitivity of neural progenitors of the subgranular zone of the dentate gyrus to irradiation is strongly exacerbated on a C57Bl6 background.

Irradiation at 10 weeks: *Ptch1*$^{+/-}$/CD1 and *Ptch1*$^{+/-}$/Bl6 mice have been irradiated with 2 Gy of γ-rays with 2 different dose-rate (0.3 Gy/min or 0.063 Gy/min) and hippocampi were collected at 4 months post-irradiation for histopathological analysis. Hippocampi were also collected from age-matched unexposed mice.

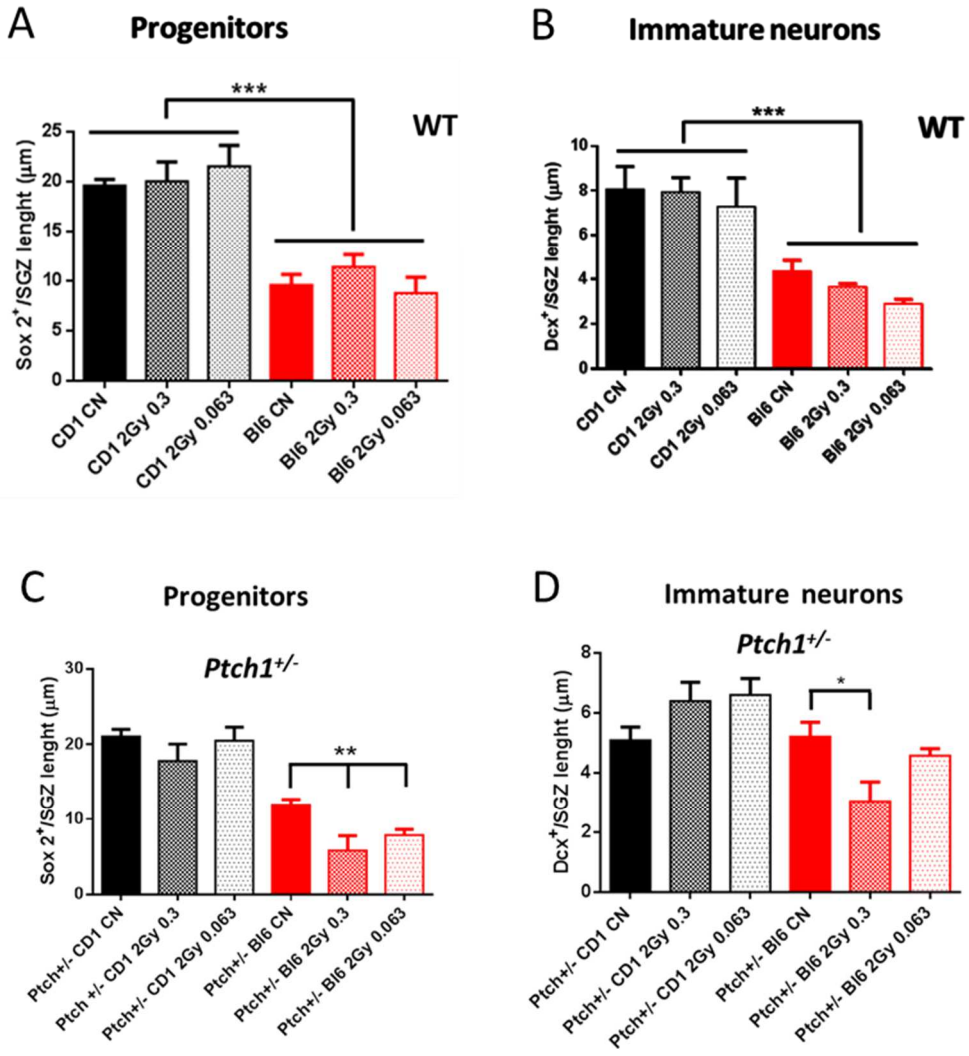

Figure 2.3: Evaluation of the effect of adult irradiation on hippocampal neurogenesis

Data for WT mice point to genetic background-related differences in the basal rate of hippocampal adult neurogenesis between the CD1 and C57BL6 control mice and complete lack of radiation effects in both mouse lines (Figure 3 A-B). Instead, in *Ptch1*$^{+/-}$ mice, we found important genetic background related differences in the long-term response of the neuronal population of the DG to irradiation. In *Ptch1*$^{+/-}$ /Bl6 mice at 4 months after irradiation with 2 Gy (0.3 Gy/min and 0.063 Gy/min), we detected a persistent impairment of Sox2 population (Figure 3 C-D). A deficit in the population of newborn neurons (Dcx+) was also detected after irradiation with 2 Gy at 0. 3 Gy/min. No alteration of neurogenesis were detected in *Ptch1*$^{+/-}$/CD1 mice.

Evaluation of lens opacity

Irradiation at P2: WT and *Ptch1*$^{+/-}$ mice (*Ptch1*$^{+/-}$/CD1, CD1, *Ptch1*$^{+/-}$/Bl6 and C57Bl6) that have been irradiated with 2 Gy of γ-rays (0.3 Gy/min) at postnatal day 2 (P2), were subjected to Scheimpflug analysis for lens opacity (Figure 4).

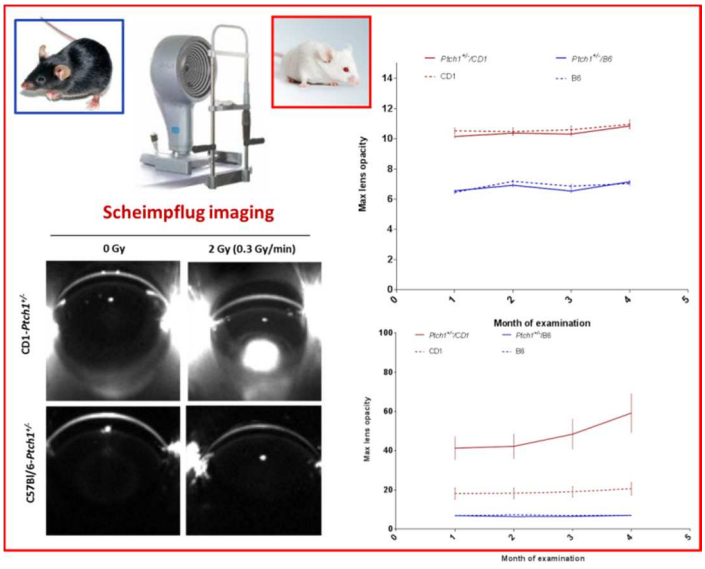

Figure 2.4: Evaluation of the effect of P2-irradiation on lens opacity through Scheimpflug analysis.

Cataract development (lens density above the LOCS III criterion of 14.1% for a type 2 cataract in humans) was exclusively induced in *Ptch1*$^{+/-}$/CD1 mice. No increase in lens opacity was found in *Ptch1*$^{+/-}$/B6 mice, indicating that induction of radiogenic cataract is strongly controlled by genetic background.

irradiation at 10W: Results produced following adult irradiation at 10W highlighted that, compared with the controls and regardless of genotype, radiation exposure is able to significantly increase the mean and maximum lens opacity, on CD1 background (Fig. 2.5A and B). Instead, no increase in lens opacity was detected in both C57Bl6-*Ptch1*$^{+/-}$ and WT mice, showing again a significant effect of genetic background (Fig. 2.5A and B).

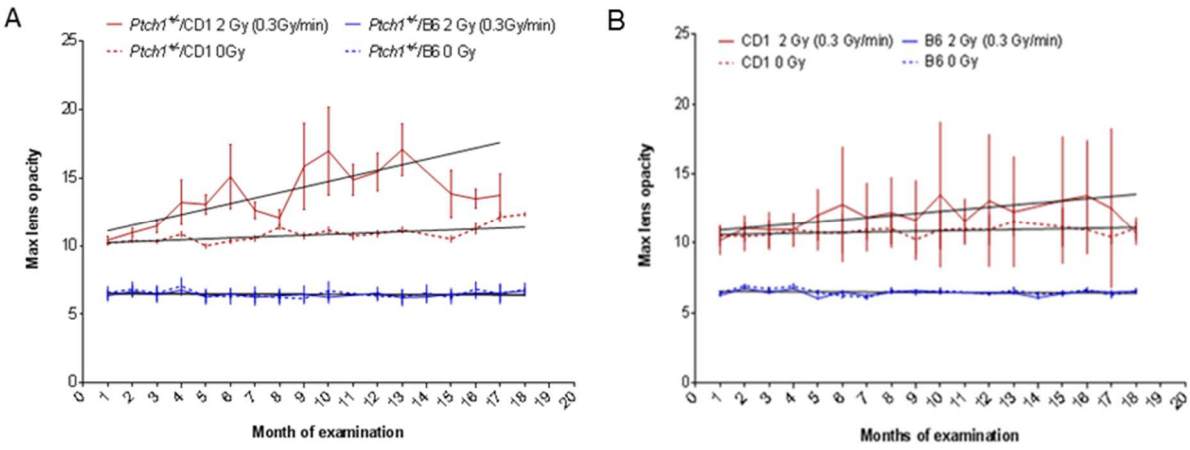

Figure 2.5: Evaluation of the effect of 10W-irradiation on lens opacity by Scheimpflug analysis.

Figure 2.6: Summary of genetic background effects on the induction of the lens and neurogenesis defects following irradiation.

3 Conclusions

Results summarized in Figure 2.6 clearly demonstrate a critical influence of the genetic background on the radiosensitivity of *Ptch1*$^{+/-}$ mice. *Ptch1*$^{+/-}$ mice on a CD1 background are highly susceptible to radiogenic cataract but resistant to impairment of hippocampal neurogenesis after irradiation. On the contrary, *Ptch1*$^{+/-}$ mice on a C57Bl6 background are resistant to the induction of radiogenic cataract but are susceptible to impairment of hippocampal neurogenesis. To elucidate the basis of genetic background driven opposite radiosensitivity, the short-term response of the lens and dentate gyrus to ionizing radiation in *Ptch1*$^{+/-}$/CD1 and *Ptch1*$^{+/-}$/C57Bl/6 mice will be assessed with a special emphasis on cell death, cellular radiosensitivity, signalling networks and DNA damage response (DDR). Overall, our data show that genetic background strongly modulates mouse radio-sensitivity by affecting the penetrance of the *Ptch1* mutation to radiation-induced defects of lens and neurogenesis both after neonatal or adult irradiation. These findings support a major contribution of individual sensitivity to the risk of radiation-induced non-cancer diseases in the population.

Further work will be needed to link the project outputs to wider work regarding low dose radiation and possible pathways for other cognitive decline processes (e.g., Alzheimer's disease and Parkinson's; e.g. https://pdfs.semanticscholar.org/4ba7/4b315f2e214bdd9f367e6cf0b0d39bd6b732.pdf).

Strain	Line	Sex	Age [mtsh.]	Dose	Dose rate	PSC	Post. Irr.	N.f. post.	ASC/Ant. lesion	Ant. Irr.	N.f. ant.	Post. Cortical irr.	n
B6C3F1	WT	m	20	0	-	0	0	6	1	0	5	0	6
	Mut	f	20	0	-	1	0	5	1	1	4	0	6
	WT	m	20	0	-	1	0	5	0	1	5	0	6
	Mut	f	20	0	-	1	2	3	1	1	4	0	6
	WT	m	20	0.5	0.3	1	0	5	1	3	2	0	6
	Mut	f	20	0.5	0.3	0	1	5	2	1	3	0	6
	WT	m	20	0.5	0.3	2	1	4	1	1	6	0	8
	Mut	f	20	0.5	0.3	2	2	2	2	1	3	0	6
	WT	m	20	1	0.3	3	1	2	4	2	0	0	6
	Mut	f	20	1	0.3	4	1	2	2	1	3	0	6
	WT	m	20	1	0.3	2	1	3	4	1	2	0	7
	Mut	f	20	1	0.3	3	0	3	2	1	3	0	6
	WT	m	20	2	0.3	6	1	0	3	1	2	0	6
	Mut	f	20	2	0.3	4	1	0	4	1	1	0	6
	WT	m	20	2	0.3	4	2	0	4	2	0	0	6
	Mut	f	20	2	0.3	5	0	1	4	1	1	0	6

Tab. 1: Findings in B6C3F1 mice. Posterior subcapsular cataracts (PSC). Posterior irregularity (Post. Irr.). No findings posterior (N.f. post.). Anterior subcapsular cataract (ASC). Anterior irregularity (Ant. Irr.). No findings anterior (N.f. ant.). Posterior cortical irregularity (Post. Cort. Irr.). Sample size (n).

Strain	Line	Sex	Age [months]	Dose	Dose rate	PSC	Post. irr.	N.f. post.	ASC/Ant. lesion	Ant. irr.	N.f. ant.	Post. Cortical irr.	n
C57BL/6J	WT	f	20	0	-	0	2	3	1	0	4	0	5
	WT	f	20	0.5	0.063	1	1	3	2	0	3	0	5
	WT	f	20	1	0.063	2	2	1	3	0	2	0	5
	WT	f	20	2	0.063	4	0	1	3	1	1	0	5
	WT	f	20	0.5	0.3	1	2	3	1	1	3	0	5
	WT	f	20	1	0.3	2	1	2	1	2	2	0	5
	WT	f	20	2	0.3	4	0	1	2	2	1	0	5
129/SV	WT	f	12	0	-	2	0	4	0	0	6	6	6
	WT	f	12	2	0.063	3	1	0	2	1	1	4	4
	WT	f	12	2	0.3	5	0	1	4	1	1	6	6

Tab. 2: Findings in C57BL/6J and 129/Sv mice. Posterior subcapsular cataracts (PSC). Posterior irregularity (Post. Irr.). No findings posterior (N.f. post.). Anterior subcapsular cataract (ASC). Anterior irregularity (Ant. Irr.). No findings anterior (N.f. ant.). Posterior cortical irregularity (Post. Cort. Irr.). Sample size (n).